



Fully coupled modeling and design of a piezoelectric actuation based valveless micropump for drug delivery application

Ranjitsinha R. Gidde¹ · Prashant M. Pawar¹ · Vishal P. Dhamgaye²

Received: 7 June 2019 / Accepted: 2 July 2019 / Published online: 10 July 2019
© Springer-Verlag GmbH Germany, part of Springer Nature 2019

Abstract

The precise control over the drug delivery involved in several vital applications including healthcare is required for achieving a therapeutic effect. For such precise control/manipulation of the drugs, micropumps are used. These micropumps are basically of two types viz. check valve-based and valveless micropumps. The valveless micropumps are preferable due to the congestion-free operation of diffuser/nozzle valves. In this paper, design optimization of a valveless piezo-electric actuation based micropump is carried out using COMSOL Multiphysics 5.0 by coupling two Multiphysics interface modules namely fluid–structure interaction and piezoelectric physics modules. Using simulation studies, the influence of pump design parameters including diffuser angle, diffuser length, neck width, chamber depth, chamber diameter and diaphragm thickness on net flow rate is studied. An optimal set of design parameters for the proposed micropump is identified. Further, the influence of actuation frequency on the flow rate is analysed. It is found that the proposed micropump is capable to deliver a net flow rate of 20 $\mu\text{l}/\text{min}$ and a maximum back pressure attainable is 200 Pa.

1 Introduction

Microfluidic systems are used in many applications, including medical testing, drug delivery, chemical analysis, chip cooling, etc. These systems have the advantages of small volume, low cost, high throughput analysis. The small fluid volumes are often pumped and controlled or otherwise manipulated in these systems (Laser and Santiago 2004). Micropumps are essential components in the microfluidic systems and are used to manipulate, transport and control the precise quantity of fluid in terms of microlitre and millilitre (Singh et al. 2015). Micropumps play a crucial role in drug delivery applications by transporting the drug from the drug reservoir to the target place with high performance, accuracy and reliability (Wang and Fu 2018). Micropumps have been developed on various principles for many different applications viz. drug delivery and biomedical assays.

Recently, various micropumps are reported which are based on different actuation mechanisms and principles

involving piezo-electric, electro-magnetic, electro-osmotic, shape memory alloy, electrostatic, etc. (Sen et al. 2007; Amirouche et al. 2009; Zhou and Amirouche 2011). Among various actuation mechanism, the piezoelectric (PZT) actuation offers several advantages such as large stroke displacement, fast response time and compact in design. However, it has a low force which can be improved by using a stack actuator. A model of valveless micropump which consists of a chamber and different diffuser designs was analyzed (Stemme and Stemme 1993). A flat walled planar design with the nozzle/diffuser arranged in the same plane as that of the pump chamber was studied (Olsson et al. 1995). The flow rate and pressure characteristics were studied using simulation as well as experiments for biometric piezoelectric pump (de Lima et al. 2009). PMMA and PDMS based micro diffuser/nozzle were fabricated and characterized for the flow and pressure profiles across the elements (Chen et al. 2003, 2008). The micropump performance characteristics have been investigated with respect to dimensions, membrane and actuator materials using the multi-field analysis with ANSYS CFX (Nisar et al. 2008). An experimental study of nozzle/diffuser micropump design using some novel non-moving-part valves was carried out to find an improved design of nozzle/diffuser valves (Yang et al. 2012). The driving performance of the piezoelectric actuator has been simulated using ANSYS software, and the relationship

✉ Ranjitsinha R. Gidde
ranjitsinhag1@rediffmail.com

¹ SVERI's College of Engineering, Pandharpur, Maharashtra, India

² Raja Ramanna Centre for Advanced Technology, Indore, Madhya Pradesh, India

between structural parameters and center displacement/frequency of piezoelectric actuator have been obtained (Guo et al. 2012). PDMS based electromagnetically actuated valveless micropump was fabricated and detailed analysis of the magnetic actuation force and the flow rate of the micropump was carried out (Yamahata et al. 2005). A shape memory alloy (SMA) actuator and PDMS elastic tube were used to realize a simple peristaltic micropump design (Sassa et al. 2012). The deflected behaviour of unimorph circular piezoelectric diaphragm actuators under electrical loading was investigated. Further, factors which affect actuators performance were thoroughly examined (Mo et al. 2006). The deflection of a circular diaphragm in case of a PZT actuator having a smaller diameter than the diaphragm was discussed (Dau et al. 2009). Valveless diaphragm micropumps employ diffuser/nozzle elements with the direction-dependent flow. Further, the diffuser efficiency and the flow rectification ability is dependent on principle dimensions of the diffuser including divergence angle, diffuser length and neck width. Hence, the shape optimization of the microfluidic pump using fluid–structure interaction (fsi) module in COMSOL Multiphysics (Pawar et al. 2016). Numerical modelling of PDMS micropump behaviour using the FSI along with viscoelastic material model which is the appropriate assumption for PDMS material was demonstrated (Gidde and Pawar 2017). Design optimization of an electromagnetic actuation-based valveless micropump for drug delivery application using fsi module and validation of optimal electromagnetic valveless micropump using experimental analysis were carried out (Gidde et al. 2019).

From the above literature survey, it is evident that simulation and experimental based analysis of piezo-electric actuation based valveless micropumps have been addressed previously by researchers. Although, considerable work on piezoelectric actuation based valveless micropump, investigations based on fully coupled electro-fluid–structural (pzd and fsi physics interface) interactions is not performed till date due to the complexities in respect of coupling two physics. This paper focuses on the investigation of piezo-electric actuation based valveless micropump to find optimal design configuration of the micropump. The proposed study is divided into six sections including problem formulation, computational formulation, simulation and parametric studies, results and discussion, limitations of the piezoelectric micropump and conclusions.

2 Problem formulation

2.1 Working principle

Figure 1 illustrates the principle of working of valveless micropump. Based on diaphragm deflection

(upward/downward), there are two modes namely supply and pump modes during one cycle. In the supply mode, the diaphragm deflects in upward direction which creates a negative pressure inside the chamber.

During this mode of operation, the fluid flows into the chamber through the inlet and outlet. However, the loss of kinetic energy in the forward direction (diffuser action) is less than that of loss of kinetic energy in the reverse direction (nozzle action). Consequently, the fluid entering from the inlet is more than the fluid entering from the outlet. Therefore, the fluid is supplied into the chamber from the inlet. During the pump mode, the diaphragm deflects in downward direction which increases the pressure of the fluid inside the chamber. As a result, the fluid from the chamber exits through the inlet and outlet. However, the fluid exiting from the outlet is more than the fluid exiting from the inlet as a result of the difference in the loss of the kinetic energy in the forward and reverse direction. Further, the difference in the pressure drop across the nozzle and diffuser elements during one cycle causes a flow rectification (Liu et al. 2011).

2.2 Optimization methodology

Micropumps' capability to transport or manipulate or control fluid in accurate volume along with the likelihood of integration with other systems depends upon design parameters viz. structural, functional and operating parameters. The structural design parameters and operating parameters are detailed in Table 1. The optimization methodology used to find the optimal values of design parameters and operating conditions is depicted in Fig. 2.

Simulations are carried out to find optimal design parameters for the valveless micropump. In this study, the effect of the principle dimensions of the diffuser element including diffuser angle, diffuser length, neck width, and pump chamber depth and chamber diameter, and thickness of diaphragm on the micropump characteristics such as flow rate and back pressure is analyzed. Finally, the micropump with the optimal parameter set of dimensions is

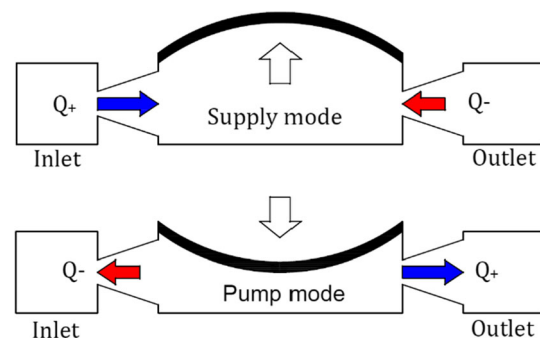


Fig. 1 Working principle of a valveless micro-pump

Table 1 Geometrical parameters and their ranges

Design variable	Bounds		Step	Unit
	Upper	Lower		
Divergence angle (2θ)	6	12	1°	°
Diffuser length (L_d)	0.8	1.4	0.1	mm
Neck width (W_n)	70	130	10	μm
Chamber depth (H)	100	400	50	μm
Chamber diameter (D_C)	7	13	1	mm
Diaphragm thickness (t_d)	75	250	25	μm

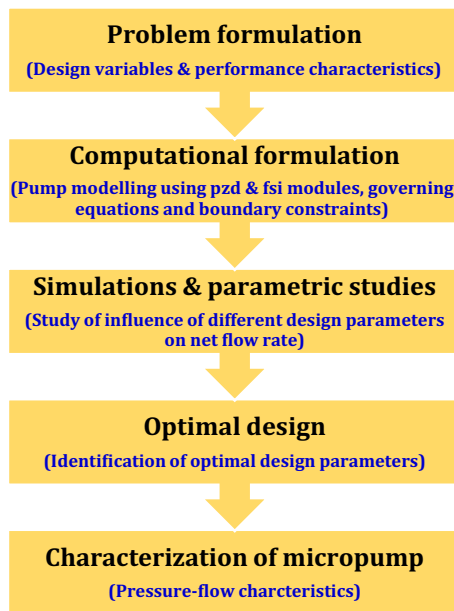


Fig. 2 Optimization methodology

studied for the flow rate and back pressure performance characteristics.

2.3 Micropump performance characteristics

To enhance the micropump performance, the number of parameters need to be optimized. The maximum flow rate and maximum back pressure are the most important output performance characteristics of the micropump. The maximum flow rate is the volume of fluid per unit time delivered by the pump at zero back pressure whereas the maximum pressure the pump can work is known as the maximum back pressure. Often, the maximum flow rate is obtained when the pump is working at zero back pressure. At the maximum back pressure, the flow rate of the pump becomes zero wherein the back pressure opposes the work done by the pump.

Flow rectification efficiency is one of the vital aspects considered in the design of a valveless micropump. It depends upon the flow in forward and reverse direction through the diffuser/nozzle element during one cycle. Accordingly, the flow rectification efficiency of the valveless micropump is expressed using Eq. (1) as given below (Singhal et al. 2004):

$$\eta_r = \frac{Q_+ - Q_-}{Q_+ + Q_-} \tag{1}$$

where η_r is the flow rectification efficiency of the micropump. Q_+ and Q_- are fluid flow in the forward direction and fluid flow in the reverse direction, respectively. Thus, the flow rectification efficiency of the micropump manifests the ability of the micropump to generate flow in a preferential direction. The flow rate is calculated using Eq. (2) as given below (Gidde et al. 2019):

$$Q_{net} = \frac{1}{2} \int_0^T Q_{outlet} - Q_{inlet} \tag{2}$$

The difference between the outlet pressure and inlet pressure is known as back pressure. In other words, back pressure or pressure head is defined as the difference between the heads at the outlet and the inlet (Nguyen and Wereley 2006).

$$h_{max} = Z_{outlet} - Z_{inlet} \tag{3}$$

2.4 Piezoelectric actuator

Piezoelectric materials generate electrical charge when stress is applied known as direct piezoelectric effect and mechanical strain when an electrical field is applied known as converse piezoelectric effect. PZT actuators convert electrical voltage into mechanical displacement. PZT actuators are divided in three basic categories namely, axial actuators (mode: d_{33}), transversal actuators (mode: d_{31}), flexural actuators (mode: d_{31}). These actuators are used as vital components in various electromechanical systems. On the basis of application, the actuator configuration can vary greatly. Axial and transversal piezoelectric actuators have high stiffness and can be optimized for controlled movements and high forces.

In case of transversal piezoelectric actuators, electrical field/charge is applied in thickness direction and mechanical strain/stress in direction of plane is produced (Kanda et al. 2017). This converse piezoelectric effect is utilized for actuating micropump diaphragm. Displacement in radial direction occurs when voltage is applied to an actuator. When this displacement is blocked, a blocking force (a measure of the stiffness of actuator) is developed. As a result of this blocking force, diaphragm gets deflected

in upward and downward direction during suction and pump mode of the micropump. Figure 3 shows a schematic of piezoelectric actuator composed of a PZT layer, a brass substrate, glue/epoxy layer and a PDMS diaphragm.

3 Computational formulation

The brief description of the numerical modelling of the piezoelectric valveless micropump is described in this section. COMSOL Multiphysics 5.0 was used to model the piezoelectric valveless micropump which is capable of performing fluid flow analysis using piezoelectric (pzd) and fluid–structure interaction (fsi) Multiphysics interface modules.

3.1 Model geometry

The schematics of a piezoelectric actuation based valveless micropump is presented in Fig. 4. The depth of the pump chamber and the nozzle-diffuser elements is H . A piezoelectric actuator comprises different elements namely a brass disc of thickness t_{br} as supporting layer and piezo element of thickness t_{pzt} and diameter d_{pzt} which is glued to the diaphragm using epoxy glue layer of thickness t_e .

3.2 Governing equation

The two physics interface modules namely, piezoelectric devices (pzd) for the electro-structural parts and fluid–structure interaction (fsi) for fluid and structure domains, (Revathi and Padmanabhan 2016) respectively were used to model the whole piezoelectric actuation based valveless micropump. The piezoelectric actuator consists of the piezoelectric disc and the thin elastic plate of brass material. Using AC voltage, the radial strain is generated in a piezoelectric disc which will cause the surface of the brass plate glued with the piezoelectric disc to bend. Consequently, deflection occurs in the PDMS diaphragm of a valveless micropump. The magnitude of deflection of

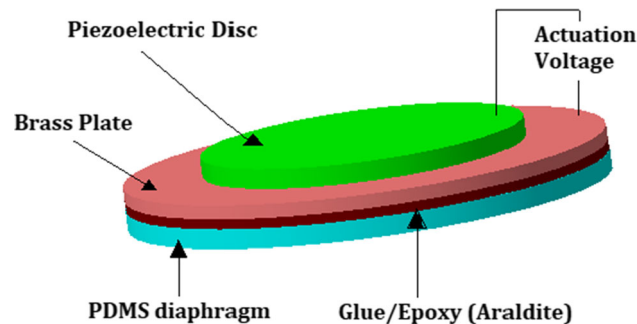


Fig. 3 Schematic of three dimensional piezoelectric actuator

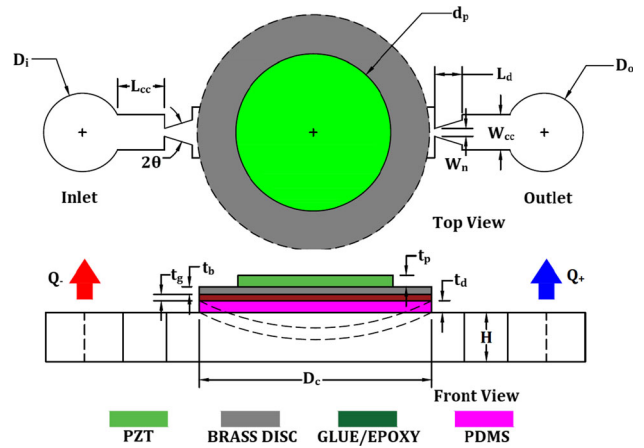


Fig. 4 Schematic of front view and top view of a piezoelectric actuation based valveless micropump

diaphragm is small in comparison with its diameter. Hence, it is governed by small deflection theory of plates. The governing equation of the transverse deflection for the elastic pump diaphragm can be expressed as (Cui et al. 2008).

$$D_f \nabla^4 W + \rho_d \frac{\partial^2 W}{\partial t^2} = f_{act} - P \tag{4}$$

where,

$$D_f = \frac{Et_d^3}{12(1 - \nu^2)} \tag{5}$$

D_f is the flexural stiffness, ∇^4 is the 2-dimensional double Laplacian operator, E is the Elastic modulus, ν is the Poisson's ratio of the diaphragm material, t_d is the thickness of the diaphragm, and ρ_d is the density of the diaphragm material. f_{act} is the periodic actuating force due to the strain of the actuator, and P is the dynamic pressure exerted on the diaphragm by the liquid. In this case, the pump diaphragm is assumed to be clamped to the brass plate. The flow is considered as an incompressible laminar flow, which can be described using the Navier–Stokes Eq. (6) and the mass continuity Eq. (7) (Fan et al. 2005).

$$\rho_f \frac{D\vec{V}}{Dt} = \rho_f \vec{g} + \mu \nabla^2 \vec{V} - \nabla P \tag{6}$$

$$\frac{\partial \rho_f}{\partial t} + (\vec{V} \cdot \nabla) \rho_f = 0 \tag{7}$$

where, ρ_f is the density of the liquid; \vec{V} is the velocity vector; μ is the viscosity of the liquid.

3.3 Boundary conditions

The fixed and zero displacement boundary conditions were applied at the edges of the diaphragm. To ensure zero relative motion at the interface between the diaphragm,

layer of epoxy glue, brass disc and PZT element the “always bonded boundary condition” has been employed. The PZT element is actuated using a sinusoidal voltage (Singh et al. 2015).

$$V(t) = V_o \sin(2\pi f_{act}t) \tag{8}$$

The pressure boundary condition is employed at both inlet and outlet, and a no-slip boundary condition is applied at the walls. The working fluid used for the simulation is assumed to be incompressible, and the flow of fluid within the micropump is assumed as laminar one.

4 Simulation and parametric studies

A detailed discussion on the grid independency test, micropump operation, flow rectification, influence of design parameters on the flow rate, response of optimal design configuration of micropump to the pressure flow characteristics and influence of voltage on the flow rate are described in this section. Three-dimensional simulations of the piezoelectric simulations are performed using pzd and fsi interface modules to determine the optimal set of dimensions and the operating conditions. The two domains namely, structural domain and fluid domain were coupled and meshed using grid system consisting of hexahedral elements. Simulations were run for few cycles to confirm about cycle-to-cycle variation in performance characteristics of the micropump. The grid independency test was carried out for the base model with the dimensions depicted in Table 2. Accordingly, results of the diaphragm deflection and flow rate at sinusoidal voltage of 50 V (peak-to-peak) and actuation frequency of 100 Hz were compared.

Four grid refinement levels were compared during grid independency test and the comparison is shown in Table 3. The error is estimated by using Eq. (9) (Xia et al. 2016).

$$\% \text{ error} = \left| \frac{F_2 - F_1}{F_1} \right| \times 100 \tag{9}$$

where F_1 is the value of diaphragm deflection/net flow rate for the finest grids and F_2 is the value of diaphragm deflection/net flow rate for other grids. It can be observed that the % errors for diaphragm deflection and net flow rate are 0.06% and 0.34%, respectively between grid systems 3 and 4. Based on this, the grid composed by hexahedral elements having maximum size and minimum size of 0.116 mm and 0.0125 mm, respectively was used to carry out simulations.

Figure 5 shows deflection contours of the diaphragm across its diameter i.e. transient analysis at 0.0025 s and 0.0075 s during supply mode and pump mode wherein maximum deflection of the diaphragm occurs. Here, the diaphragm deflection is maximum at the center and zero at

the edges as expected conceptually. During the supply mode, the diaphragm deflects in upward direction and fluid enters from both inlet and outlet through diffuser elements. During the pump mode, the diaphragm deflects in downward direction and subsequently fluid exits from the inlet and outlet through diffuser elements.

It can be observed from Fig. 6 that the fluid entering through diffuser/nozzle element at the inlet during the supply mode is more than that of the flow exiting during the pump mode as a result of flow rectification caused as a result of difference in the pressure drop across nozzle and diffuser elements.

The variation in deflection of diaphragm as a function of time at 50 V with 100 Hz actuating frequency i.e. transient response of diaphragm deflection for two cycles is represented in Fig. 7. It is noted that the diaphragm deflection is more in supply mode as compared to the diaphragm deflection in pump mode. The maximum diaphragm deflection is 2.4966 μm at 0.0025 s during supply mode. However, its magnitude is slightly decreased during pump mode and is 2.4891 μm at 0.0075 s. This decrease in maximum diaphragm deflection during pump mode is due to the presence of the fluid within the pump chamber. Additionally, the flow rectification can be clarified with the help of the transient response of flow rate through inlet and outlet during supply and pump modes as shown in Fig. 8. It clearly reveals that during the supply mode (Time period: 0 to 0.005 s), the fluid entering through the inlet (Q_+) into the pump chamber is more than the fluid entering through the outlet (Q_-) into the pump chamber. In contrast, during the pump mode (Time period: 0.005 to 0.01 s), the fluid leaving through the outlet (Q_+) is more than that of the fluid leaving through the inlet (Q_-).

4.1 Influence of parameters on the flow rate

The influence of the various design parameters on the net flow rate needs to be studied to identify the optimal design parameters for the micropump. Hence, the response of the various design parameters to the net flow rate is discussed in this section.

The flow rate as a function of divergence angle is represented as shown in Fig. 9a. It can be observed that for the smaller values of divergence angle, the flow rectification through diffuser element is low as resistance offered by nozzle and diffuser is same. The net flow rate increases with increase in the value of divergence angle. This trend is continued up to $2\theta \leq 9$ for the range of divergence angle studied here (6° to 12°).

However, at much higher divergence angles, i.e. $2\theta > 9^\circ$, a decrease in the net flow rate occurs which may be due to the flow separation. Hence, the divergence angle of 9° is found to be optimum. The influence of the diffuser

Table 2 Physical and geometrical parameters of the piezoelectric valveless micropump employed in simulations

Sr. no.	Component/material	Parameter/variable	Value	Unit
(A) Functional layer and diaphragm: base model				
1.	Pump chamber	Diameter (D_c)*	12	mm
2.	Diffuser element	Divergence angle (2θ)*	10	°
		Diffuser length (L_d)*	1.3	mm
		Neck width (W_n)*	100	μm
3.	Constriction channel	Length (L_{cc})	2.0	mm
		Width (W_{cc})	600	μm
4.	Inlet/Outlet	Diameter ($D_i = D_o$)	2.0	mm
5.	Functional layer	Chamber Depth (H)*	250	μm
6.	PDMS diaphragm	Diameter (D_d)	12	mm
		Thickness (t_d)*	150	μm
7.	Glue/Epoxy (Araldite) layer	Diameter (D_g)	12	mm
		Thickness (t_g)	80	μm
(B) Piezoelectric actuator				
1.	Brass plate	Diameter (D_{br})	12	mm
		Thickness (t_{br})	120	μm
2.	PZT-5A disc	Diameter (D_p)	8.00	mm
		Thickness (t_p)	140	μm
(C) Mechanical properties				
1.	PZT-5A ($PbZrTiO_3$)	Compliance matrix	$\begin{bmatrix} 16.4 & -5.74 & -7.22 & 0 & 0 & 0 \\ -5.74 & 16.4 & -7.22 & 0 & 0 & 0 \\ -7.22 & -7.22 & 18.8 & 0 & 0 & 0 \\ 0 & 0 & 0 & 47.5 & 0 & 0 \\ 0 & 0 & 0 & 0 & 47.5 & 0 \\ 0 & 0 & 0 & 0 & 0 & 44.3 \end{bmatrix} \times 10^{-12}$	(m^2/N)
		Coupling matrix	$\begin{bmatrix} 0 & 0 & -171 \\ 0 & 0 & -171 \\ 0 & 0 & 374 \\ 0 & 584 & 0 \\ 584 & 0 & 0 \\ 0 & 0 & 0 \end{bmatrix} \times 10^{-12}$	(C/N)
		Relative permittivity	$\begin{bmatrix} 1730 & 0 & 0 \\ 0 & 1730 & 0 \\ 0 & 0 & 1700 \end{bmatrix}$	–
		Young's modulus	63×10^3	(MPa)
		Poisson's ratio	0.30	–
		Density	7700	(kg/m^3)
2.	Brass	Young's modulus	90×10^3	(MPa)
		Poisson's ratio	0.32	–
		Density	8500	(kg/m^3)
3.	Glue/epoxy (araldite)	Young's modulus	979	(MPa)
		Poisson's ratio	0.30	–
		Density	1500	(kg/m^3)
4.	PDMS diaphragm	Young's modulus	0.8	(MPa)
		Poisson's ratio	0.49	–
		Density	965	(kg/m^3)
5.	Water	Density	997	(kg/m^3)
		Kinematic viscosity	0.0014	kg/m s
(D) Operational conditions				

Table 2 (continued)

Sr. no.	Component/material	Parameter/variable	Value	Unit
1.	Piezoelectric actuator	Alternating voltage (Vpp)**	50	V
		Actuation frequency	100	Hz

*Indicates design variables used to find optimal design of micropump

**Indicates peak-to-peak voltage

length, L_d on the net flow rate is shown in Fig. 9b. The deviation in flow resistance between the nozzle and diffuser elements is less at lower values of diffuser length, L_d . This results in very low flow rectification accordingly the net flow rate is decreased. In line with this, the pressure drop also increases at higher values of L_d . Consequently, the net flow rate starts decreasing beyond diffuser length of 1.2 mm. Hence, the optimum nozzle-diffuser length L_d is 1.2 mm. The influence of the neck width, W_n on the net flow rate is shown in Fig. 9c. The net flow rate is found to be less at lower values as well as at the higher values of neck width. This trend in net flow rate is due to the choking effect at lower values of neck width and flow separation effect at higher values of neck width. Hence, the optimal value of the neck width is 100 μm .

Pump chamber diameter and depth are the two critical geometrical parameters which affect flow rate capability of the mechanical micropump. The response of the chamber depth, H to the net flow rate has been studied by varying the chamber depth in the range 100–400 μm in the step of 50 μm as shown in Fig. 9d. The flow rate increases with the increase in chamber depth up to specific value due to the reduction in the flow losses. However, larger chamber depth prevents complete transfer of energy from the diaphragm into the fluid present in the pump chamber due to the increased damping characteristic as a result of more fluid. Here, flow rate reduces with increase in the chamber depth beyond 300 μm . The response of pump chamber diameter on the net flow rate is depicted in Fig. 9e. An increase in the chamber diameter also improves the flow rate due to increase diaphragm’s swept volume. It can be clarified using Eq. (10) as given below (Singh et al. 2015):

$$\Delta V = \frac{\pi}{6} W_o D_c^2 \tag{10}$$

where, W_o denotes the total maximum deflection of the diaphragm. In order to minimize the dead volume, pump chamber diameter should be kept minimum (Nguyen and Wereley 2002).

It is important to note that the pump chamber diameter cannot increase beyond particular limit due to certain space and size related constraints which in turn limits the size of the micro-devices. Further, small diameter facilitates pump to be used in Lab on a Chip application. Hence, for

proposed design, the optimal pump chamber diameter is 12 mm.

The net flow rate as a function of diaphragm thickness is presented in Fig. 9(f). The diaphragm thickness has linear relationship with the net flow rate, i.e. with increase in diaphragm thickness, the net flow rate decreases. This is due to the fact that the deflection of the diaphragm reduces with the increase in the thickness as the thicker diaphragm has more resistance to deflect. Further, it is well known that the swept volume of the diaphragm is a function of diaphragm deflection which in turn determines the amount of fluid pumped. However, diaphragm thickness cannot reduce beyond a certain limit due to the problems arising from self-sagging and stiction of the diaphragm surface (Mohith et al. 2018) and it would be difficult to manufacture thin diaphragm of thickness around 100 μm and also it would be to handle as well. There may be possibility of reliability issues under fatigue conditions. Hence, in the proposed micropump design, the thickness of the diaphragm is selected to be 150 μm .

4.2 Optimal micropump design configuration

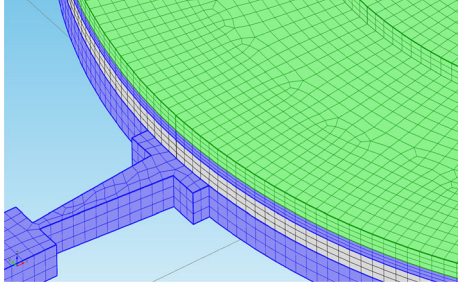
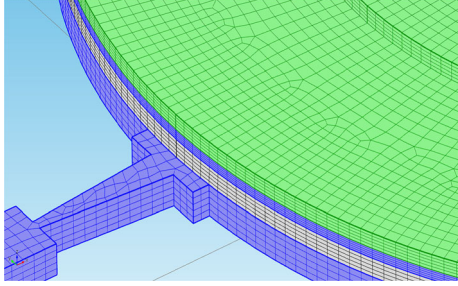
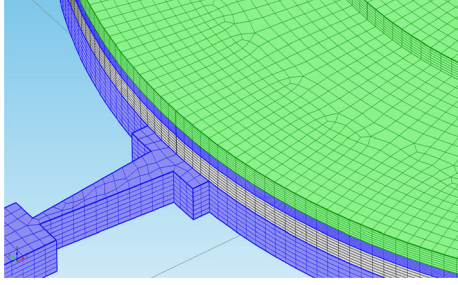
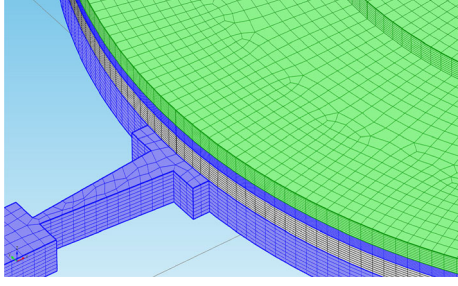
In the previous section, the influence of micropump’s geometrical parameters on the net flow rate is analysed. The optimal and other fixed design parameters used to carry out characterization of the micropump are given in Table 4.

The two performance characteristics namely, the net flow rate and the back pressure are used to characterize the performance of the micropump. In fact, the influence of the actuation frequency on the net flow rate needs to be studied to determine the required operating conditions. It is required to achieve the desired flow for particular microfluidics application.

4.3 Pressure flow characteristics

The flow rate delivered by micropump is dependent on the various geometrical as well as operating parameters including the ratio of actuating frequency and natural frequency of the diaphragm, density of the working fluid and diaphragm, size of nozzle/diffuser elements, size of the chamber and size of the diaphragm. The resonant

Table 3 Grid independency test at actuating voltage and frequency of 50 V and 100 Hz, respectively for diaphragm deflection and flow rate

Sr. no.	Grid system with hexahedral elements	Number of elements	Deflection (μm)	% error	Flow rate ($\mu\text{l}/\text{min}$)	% error
1.		1,48,713	2.5476	1.77	6.732	3.55
2.		2,47,855	2.5034	0.17	6.501	1.03
3.		3,46,997	2.4941	0.06	6.4301	0.34
4.		4,46,139	2.4966	–	6.413	–

Note: Green layers at the top indicate piezo-actuator, blue layer at the bottom indicates water domain, layer above water domain represents PDMS diaphragm and layer below piezo-actuator indicates glue

frequency of the diaphragm based micropump decrease with the nozzle/diffuser slenderness ratio and it increases with divergence angle of the diffuser/nozzle, high aspect ratio, and thickness ratio (Zhou and Amirouche 2009). Initially, at actuating voltage of 50 V (peak to peak value), the influence of actuating frequency within the range 0–175 Hz on the flow rate has been investigated.

The simulation result in terms of the flow rate as a function of actuation frequency is depicted in Fig. 10. At the beginning, the flow rate increases with the increase in the actuation frequency. The flow rate reaches a maximum

value of 20 $\mu\text{l}/\text{min}$ at an actuation frequency of 150 Hz and beyond $f_{acr} = 150$ Hz, the flow rate decreases. The trend of initial increase in the flow rate up to 150 Hz frequency can be elucidated with the help of simulation results for pressure inside the pump chamber at different actuation frequency as shown in Fig. 11. These results indicate that the pressure applied to the diaphragm and consequently pressure inside the micropump chamber increases with increase in the frequency (Singh et al. 2015). This is due to the fact that the force generated by the piezoelectric actuator

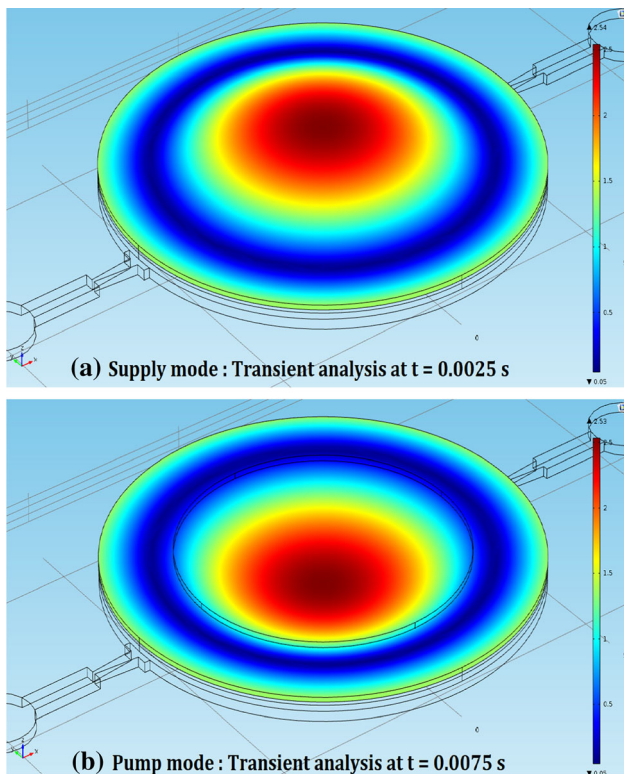


Fig. 5 Contours of diaphragm deflection across its diameter **a** upward direction and **b** downward direction

increases with the actuating frequency (Revathi and Padmanabhan 2018).

The maximum flow rate with zero back pressure is observed at the actuation frequency of 150 Hz. By keeping voltage and other parameters constant, for the actuation frequency beyond 150 Hz, the sudden decrease in the flow rate is observed. This is due to the fact that the maximum displacement of the diaphragm is much larger at the resonant frequency than at frequencies lower or higher than the resonant frequency of the actuating mechanism. This higher displacement results in higher swept volume consequently flow rate is more at 150 Hz and decreases beyond the 150 Hz. Further, small damping is observed at actuation frequency equal to the natural frequency of the actuating mechanism.

In practical applications, the flow characteristics with respect to back pressure are of significant importance and are different due to change in the layout of microfluidic systems used in different applications. Hence, the influence of back pressure on the flow rate was investigated at actuation frequency of 150 Hz and sinusoidal voltage of 50 V (peak-to-peak). The pressure flow characteristics of micropump are represented in Fig. 12. The results indicate micropump’s capability in terms of maximum flow rate and maximum back pressure. At the zero back pressure, the maximum flow rate observed is 20 $\mu\text{l}/\text{min}$, whereas a back

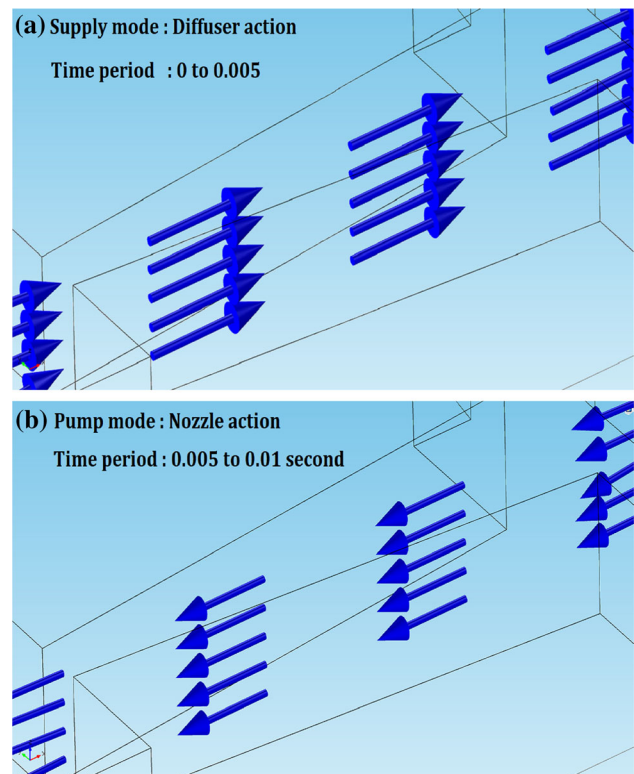


Fig. 6 Simulation results of flow through diffuser/nozzle: velocity vectors **a** the flow entering into the chamber through diffuser element (Q_+) at the inlet and **b** the flow exiting from the chamber through diffuser element (Q_-) at the inlet

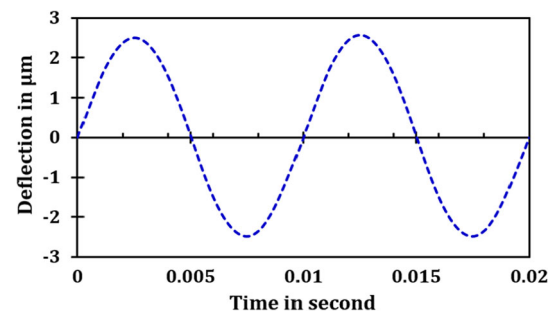


Fig. 7 Transient response: diaphragm deflection versus time during two cycles at actuation voltage of 50 V with actuation frequency of 100 Hz

pressure of 200 Pa is observed. Further, the effect of excitation voltage on the maximum flow rate and back pressure has been studied and accordingly pressure flow characteristics are represented as shown in Fig. 12.

With increasing the excitation voltage, the flow rate increases to 24 $\mu\text{l}/\text{min}$ at zero back pressure and maximum back pressure of 225 Pa can be attained. This is clarified with the help of diaphragm deflection as a function of actuation voltage shown in Fig. 13.

Here, the diaphragm deflection at actuation voltage of 70 V is higher than that of its magnitude corresponding to

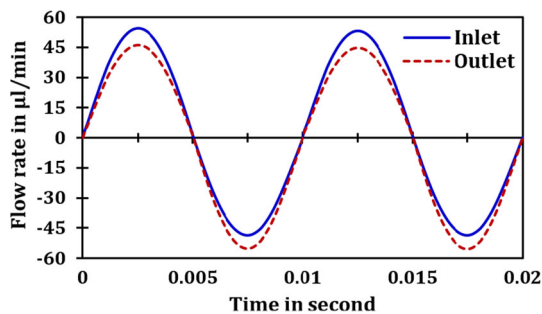


Fig. 8 Transient response: flow rate through the inlet and outlet as a function of time during two cycles at actuation voltage of 50 V with actuation frequency of 100 Hz

the 50 V. Hence, the net flow rate delivered by the micropump can be varied with respect to the application by controlling the actuation voltage to the piezo-actuator. This adjustable flow rate characteristic of the piezoelectric

micropump makes it a suitable candidate for drug-delivery applications.

5 Limitations of piezoelectric micropump

The exciting voltage of the piezoelectric actuators is proportional to the size and is limited in practical work. The displacement, force, and actuating voltage are vital parameters in case of the piezoelectric actuator (Nguyen and Truong 2004; Park et al. 2013; Pan et al. 2015; Zhang et al. 2013). Most piezoelectric diaphragm micropumps utilize a piezo disk which directly glued on the pump diaphragm. The piezo disc works in the quasi-static state. Consequently, both operating frequency and the volume change of the micropump induced by the diaphragm deflection are small. For improving the performance of piezoelectric actuators, effective methods are adopted,

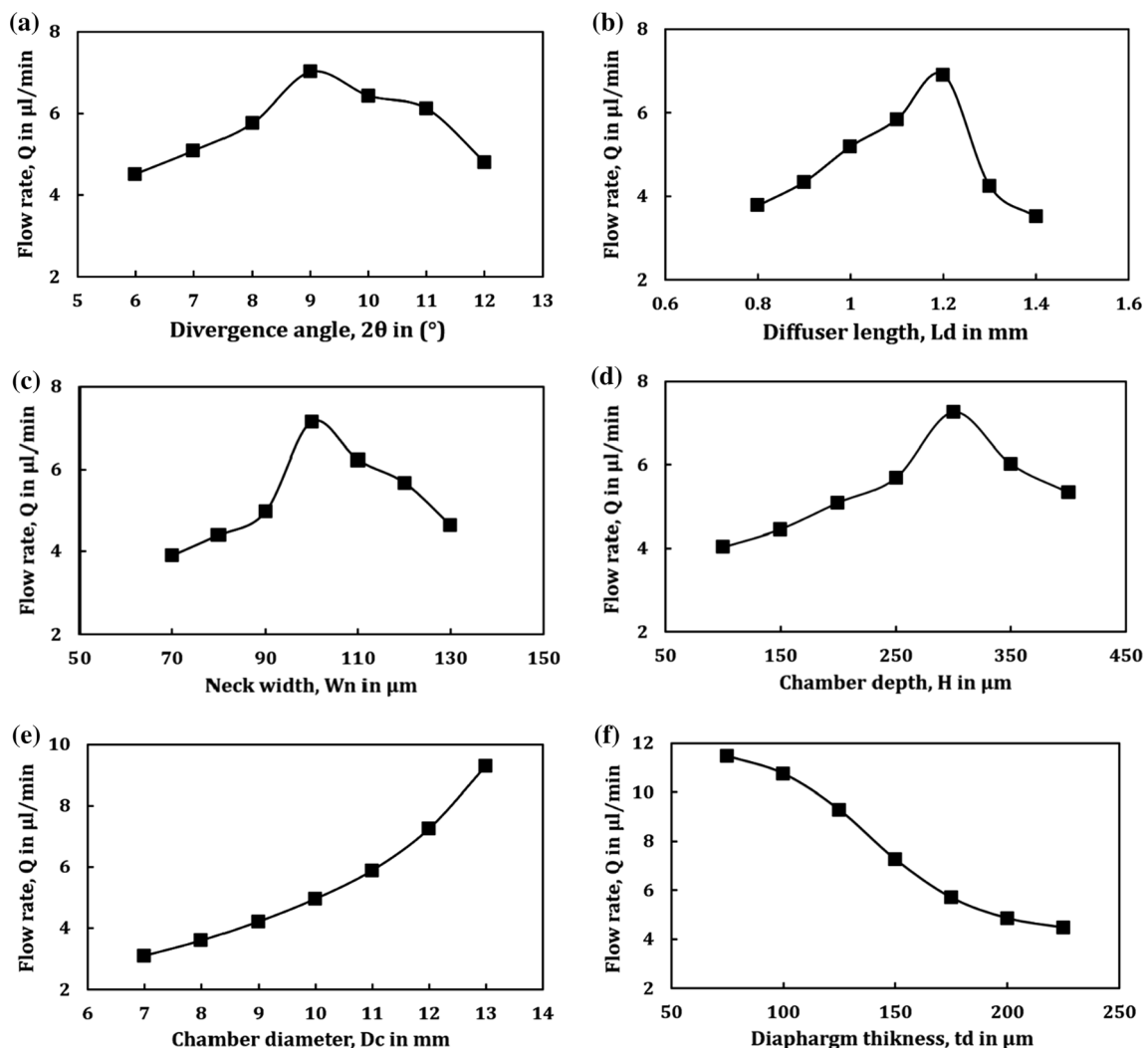


Fig. 9 Parametric studies: flow rate as a function of **a** divergence angle, **b** diffuser length, **c** neck width, **d** chamber depth, **e** chamber diameter and **f** diaphragm thickness, at actuation voltage of 50 V with actuation frequency of 100 Hz

Table 4 Optimal and fixed design parameters

Parameter	Description	Value	Unit
Optimal	Divergence angle (2θ)	9	$^\circ$
	Diffuser length (L_d)	1.2	mm
	Neck width (W_n)	100	μm
	Chamber depth (H)	300	μm
	Chamber diameter (D_C)	12	mm
	Diaphragm thickness (t_d)	150	μm
Fixed	Constriction channel length (L_{cc})	2.0	mm
	Constriction channel width (W_{cc})	600	μm
	Inlet chamber radius (D_i)	2.0	mm
	Outlet chamber radius (D_o)	2.0	mm

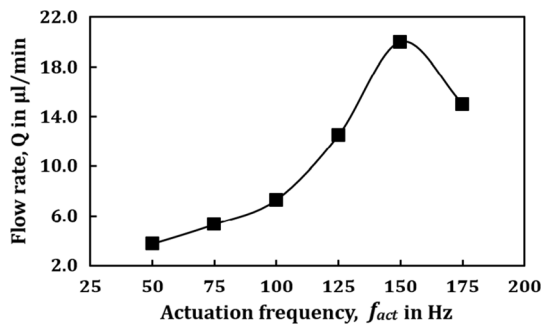


Fig. 10 Water flow rate as a function of actuation frequency at zero backpressure

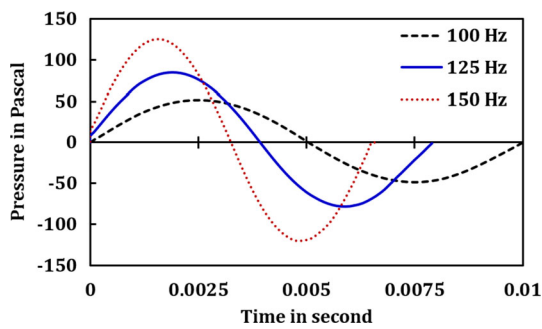


Fig. 11 Transient response: variation of pressure inside the micropump chamber as a function of actuating frequency for 100 Hz, 125 Hz and 150 Hz, respectively during one cycle

which includes increasing actuation frequency and raising the amplitude of the displacement. Consequently, enhanced performance can be achieved at a higher frequency. Another approach includes increasing the actuating voltage to increase the amplitude. However, the excitation voltage also has a limit. Hence, these micropumps require more sophisticated driver electronics.

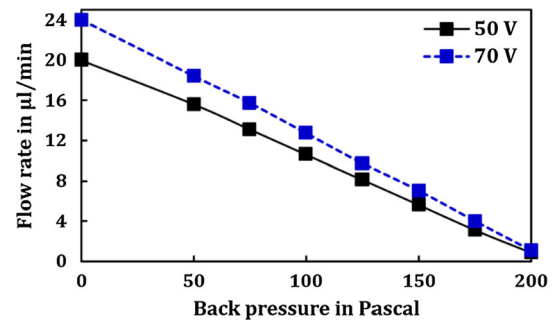


Fig. 12 Water flow rate as a function of back pressure

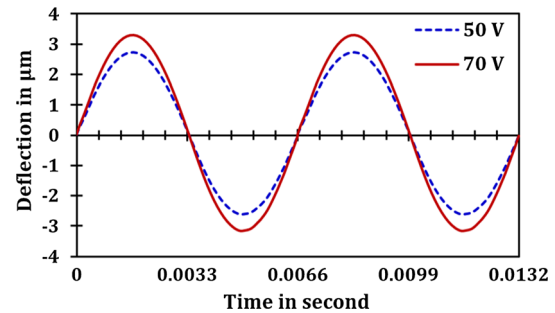


Fig. 13 Transient response: intensification in diaphragm deflection as a function of actuation voltage at constant actuating frequency of 150 Hz for two cycles

6 Conclusions

In this paper, the numerical investigation of three Dimensional piezoelectric actuation based valveless micropump is reported. It is well-intentioned that the micropump performance characteristics namely flow rate and back pressure are predominately influenced by geometrical parameters as well as operating conditions. The micropumps' performance can be enhanced through proper choice of geometrical and operating conditions.

Based on the extensive simulations performed in this study, the following conclusions are drawn which highlight the findings in respect of proposed piezoelectric actuation based valveless micropump:

1. Simulation results of velocity vectors at diffuser/nozzle configuration show that the flow entering into the pump chamber through the inlet during the supply mode is more as compared to the flow exiting the inlet during the pump mode. This represents flow rectification property of the nozzle/diffuser elements.
2. In a nutshell, it is clear that the micropump performance is affected by principal dimensions of nozzle/diffuser, pump chamber dimensions and diaphragm dimensions. There are certain threshold values of these parameters which are required for desired performance.

3. The dimensions of optimal diffuser/nozzle geometry are divergence angle = 9°, diffuser length = 1.2 mm and neck width = 0.100 mm. The optimal chamber depth is found to be 300 μm. On the basis of space and size constraints of Microfluidic Chip/Lab on a Chip devices, the specified values for chamber diameter and diaphragm thickness are 12 mm and 150 μm, respectively.
4. The initial increment in flow rate with respect to actuation frequency up to the fundamental frequency of an optimal micropump design configuration has been observed. This increase has been clarified in terms of increase in pressure inside the pump chamber with increase in the frequency from 100 to 150 Hz.
5. On the basis of simulation results, for optimal design configuration, the maximum flow rate observed is 20 μl/min when operating at actuation voltage and actuation frequency of 50 V and 150 Hz, respectively with zero back pressure. Further, the micropump is capable to attain the maximum back pressure of 200 Pa.
6. For the actuation voltage and actuation of frequency of 70 V and 150 Hz, respectively, the maximum flow rate observed is 24 μl/min at zero back pressure and the maximum back pressure of 225 Pa is attained. This intensification in micropump's characteristics is due to increase in diaphragm's deflection, which in turn results in higher swept volume.
7. Voltage-based flow rate characteristics facilitate its suitability for drug delivery applications.

7 Future studies

In this regards, an attempt can be made to understand effect of diaphragm material, design, geometry and loading method on the pressure flow characteristics.

References

- Amirouche F, Zhou Y, Johnson T (2009) Current micropump technologies and their biomedical applications. *Microsyst Technol* 15(5):647–666
- Chen YT, Kang SW, Chang PF (2003) A manufacturing technique for 3D polymer micro-venturi tube. *Int J Mach Tools Manuf* 43(4):421–424
- Chen YT, Kang SW, Wu LC, Lee SH (2008) Fabrication and investigation of PDMS micro-diffuser/nozzle. *J Mater Process Technol* 198(1–3):478–484
- Cui Q, Liu C, Zha XF (2008) Simulation and optimization of a piezoelectric micropump for medical applications. In *J Adv Manufact Technol* 36(5–6):516–524
- Dau VT, Dinh TX, Katsuhiko T, Susumu S (2009) A cross-junction channel valveless-micropump with PZT actuation. *Microsyst Technol* 15(7):1039–1044
- de Lima CR, Vatanabe SL, Choi A, Nakasone PH, Pires RF, Silva ECN (2009) A biomimetic piezoelectric pump: computational and experimental characterization. *Sens Actuators A* 152(1):110–118
- Fan B, Song G, Hussain F (2005) Simulation of a piezoelectrically actuated valveless micropump. *Smart Mater Struct* 14(2):400
- Gidde RR, Pawar PM (2017) On effect of viscoelastic characteristics of polymers on performance of micropump. *Adv Mech Eng* 9(2):1687814017691211
- Gidde RR, Pawar PM, Ronge BP, Dhamgaye VP (2019) Design optimization of an electromagnetic actuation based valveless micropump for drug delivery application. *Microsyst Technol* 25(2):509–519
- Guo L, Yan W, Xu Y, Chen Y (2012) Valveless piezoelectric micropump of parallel double chambers. In *J Precis Eng Manuf* 13(5):771–776
- Kanda K, Moriue S, Fujita T, Maenaka K (2017) Three-dimensional piezoelectric MEMS actuator by using sputtering deposition of Pb (Zr, Ti) O₃ on microstructure sidewalls. *Smart Mater Struct* 26(4):045019
- Laser DJ, Santiago JG (2004) A review of micropumps. *J Micromech Microeng* 14(6):R35
- Liu Y, Komatsuzaki H, Imai S, Nishioka Y (2011) Planar diffuser/nozzle micropumps with extremely thin polyimide diaphragms. *Sens Actuators A* 169(2):259–265
- Mo C, Wright R, Slaughter WS, Clark WW (2006) Behaviour of a unimorph circular piezoelectric actuator. *Smart Mater Struct* 15(4):1094
- Mohith S, Karanth PN, Kulkarni SM (2018) Recent trends in mechanical micropumps and their applications: a review. *Mechatronics* 60:34–55
- Nguyen NT, Truong TQ (2004) A fully polymeric micropump with piezoelectric actuator. *Sens Actuators B Chem* 97(1):137–143
- Nguyen NT, Wereley S (2006) Fundamentals and applications of microfluidics. Artech house, pp 293–341
- Nisar A, Afzulpurkar N, Mahaisavariya B, Tuantranont A (2008) MEMS-based micropumps in drug delivery and biomedical applications. *Sens Actuators B Chem* 130(2):917–942
- Olsson A, Stemme G, Stemme E (1995) A valve-less planar fluid pump with two pump chambers. *Sens Actuators A* 47(1–3):549–556
- Pan QS, He LG, Huang FS, Wang XY, Feng ZH (2015) Piezoelectric micropump using dual-frequency drive. *Sens Actuators A* 229:86–93
- Park JH, Seo MY, Ham YB, Yun SN, Kim DI (2013) A study on high-output piezoelectric micropumps for application in DMFC. *J Electroceram* 30(1–2):102–107
- Pawar PM, Gidde RR, Ronge BP (2016) Shape optimization of microfluidic pump using fluid-structure interaction approach. In: *techno-societal 2016, international conference on advanced technologies for societal applications*. Springer, Cham, pp 471–477
- Revathi S, Padmanabhan R (2016) Study of the effect on flow rate for planar type polymer-based diaphragm piezoelectric actuated valveless micropump for insulin delivery. *Adv Mater Proc Technol* 2(1):31–43
- Revathi S, Padmanabhan R (2018) Design and Development of piezoelectric composite-based micropump. *J Microelectromech Syst* 27(6):1105–1113
- Sassa F, Al-Zain Y, Ginoza T, Miyazaki S, Suzuki H (2012) Miniaturized shape memory alloy pumps for stepping microfluidic transport. *Sens Actuators B Chem* 165(1):157–163

- Sen AK, Darabi J, Knapp DR (2007) Simulation and parametric study of a novel multi-spray emitter for ESI-MS applications. *Microfluid Nanofluid* 3(3):283–298
- Singh S, Kumar N, George D, Sen AK (2015) Analytical modeling, simulations and experimental studies of a PZT actuated planar valveless PDMS micropump. *Sens Actuator A Phys* 225:81–94
- Singhal V, Garimella SV, Murthy JY (2004) Low Reynolds number flow through nozzle-diffuser elements in valveless micropumps. *Sens Actuator A Phys* 113(2):226–235
- Stemme E, Stemme G (1993) A valveless diffuser/nozzle-based fluid pump. *Sens Actuator A Phys* 39(2):159–167
- Wang YN, Fu LM (2018) Micropumps and biomedical applications—a review. *Microelectron Eng* 195:121–138
- Xia GD, Li YF, Wang J, Zhai YL (2016) Numerical and experimental analyses of planar micromixer with gaps and baffles based on field synergy principle. *Int Commun Heat Mass Transf* 71:188–196
- Yamahata C, Lotto C, Al-Assaf E, Gijs MAM (2005) A PMMA valveless micropump using electromagnetic actuation. *Microfluid Nanofluid* 1(3):197–207
- Yang KS, Chao TF, Chen IY, Wang CC, Shyu JC (2012) A comparative study of nozzle/diffuser micropumps with novel valves. *Molecules* 17(2):2178–2187
- Zhang Z, Kan J, Cheng G, Wang H, Jiang Y (2013) A piezoelectric micropump with an integrated sensor based on space-division multiplexing. *Sens Actuators A Phys* 203:29–36
- Zhou Y, Amirouche F (2009) Study of fluid damping effects on resonant frequency of an electromagnetically actuated valveless micropump. *Int J Adv Manuf Technol* 45(11–12):1187
- Zhou Y, Amirouche F (2011) An electromagnetically-actuated all-PDMS valveless micropump for drug delivery. *Micromachines* 2(3):345–355

Publisher's Note Springer Nature remains neutral with regard to jurisdictional claims in published maps and institutional affiliations.